JAEA-Research
2021-011
DOI:10.11484/jaea-research-2021-011

JAEA-Research

Effect of Nitrous Acid on Migration Behavior of Gaseous Ruthenium Tetroxide into Liquid Phase

Naoki YOSHIDA, Takuya ONO, Ryoichiro YOSHIDA, Yuki AMANO and Hitoshi ABE

Fuel Cycle Safety Research Division
Nuclear Safety Research Center
Sector of Nuclear Safety Research and Emergency Preparedness

January 2022

Japan Atomic Energy Agency

日本原子力研究開発機構

国立研究開発法人日本原子力研究開発機構　JAEA イノベーションハブ　研究成果利活用課
〒 319-1195　茨城県那珂郡東海村大字白方 2 番地 4
電話 029-282-6387, Fax 029-282-5920, E-mail:ird-support@jaea.go.jp

Institutional Repository and Utilization Section, JAEA Innovation Hub,
Japan Atomic Energy Agency.
2-4 Shirakata, Tokai-mura, Naka-gun, Ibaraki-ken 319-1195 Japan
Tel +81-29-282-6387, Fax +81-29-282-5920, E-mail:ird-support@jaea.go.jp

Effect of Nitrous Acid on Migration Behavior of Gaseous Ruthenium Tetroxide into Liquid Phase

Naoki YOSHIDA, Takuya ONO, Ryoichiro YOSHIDA, Yuki AMANO and Hitoshi ABE

Fuel Cycle Safety Research Division, Nuclear Safety Research Center
Sector of Nuclear Safety Research and Emergency Preparedness
Japan Atomic Energy Agency
Tokai-mura, Naka-gun, Ibaraki-ken

(Received November 4, 2021)

In boiling and drying accidents involving high-level liquid waste in fuel reprocessing plants, emphasis is placed on the behavior of ruthenium (Ru). Ru would form volatile species, such as ruthenium tetroxide (RuO_4), and could be released to the environment with coexisting gases, including nitric acid, water, or nitrogen oxides. In this study, to contribute toward safety evaluations of these types of accidents, the migration behavior of gaseous Ru into the liquid phase has been experimentally measured by simulating the condensate during an accident. The gas absorption of RuO_4 was enhanced by increasing the nitrous acid (HNO_2) concentration in the liquid phase, indicating the occurrence of chemical absorption. In control experiments without HNO_2, the lower the temperature, the greater was the Ru recovery ratio in the liquid phase. Conversely, in experiments with HNO_2, the higher the temperature, the higher the recovery ratio, suggesting that the reaction involved in chemical absorption was activated at higher temperatures.

Keywords: Nuclear Fuel Cycle Facility, Boiling and Drying, Ruthenium, Ruthenium Tetroxide, Severe Accident

気体状四酸化ルテニウムの液相への移動挙動に及ぼす亜硝酸の影響

日本原子力研究開発機構　安全研究・防災支援部門 安全研究センター
燃料サイクル安全研究ディビジョン
吉田 尚生、大野 卓也、吉田 涼一朗、天野 祐希、阿部 仁

（2021 年 11 月 4 日受理）

再処理施設における高レベル濃縮廃液の蒸発乾固事故について、ルテニウム (Ru) の挙動が着目されている。Ru は四酸化ルテニウム (RuO_4) のような揮発性の化学種を形成し、硝酸、水または窒素酸化物を含む共存ガスと共に施設外へ放出される可能性があるためである。本研究では、蒸発乾固事故に対する安全性評価に資することを目的として、事故時の蒸気凝縮を模擬した、水溶液に対する気体状 RuO_4 の液相への移行挙動を実験的に測定した。その結果、RuO_4 のガス吸収は液相中の亜硝酸 (HNO_2) 濃度の増加により促進されたことから、化学吸収を伴う物質移動であることが示唆された。HNO_2 を用いない対照実験では、温度が低いほど液相中の Ru 吸収率は大であったのに対し、HNO_2 を用いた実験では、温度が高いほど Ru 吸収率が高かった。これは化学吸収に関与する化学反応が高温で活性化されたためであると考察される。

原子力科学研究所：〒319-1195 茨城県那珂郡東海村大字白方 2-4

Contents

目　次

This is a blank page.

1. Introduction

A severe accident possible in nuclear waste reprocessing plants is evaporation to dryness due to the loss of cooling functions (EDLCF) [1)]. High-level liquid waste contains fission products that are removed during reprocessing and must be cooled constantly because they generate decay heat. In EDLCF accidents, it has been reported that ruthenium (Ru) is released into the gas phase at a higher rate than other elements because it forms volatile compounds, such as ruthenium tetroxide (RuO_4) [2,3)]. Hence, it is essential to know the migration of gaseous Ru for safety studies on EDLCF and for consideration of mitigation measures.

In EDLCF, gaseous Ru is released with coexisting gases, such as water (H_2O) vapor, nitric acid (HNO_3) vapor, and nitrogen oxides (NO_x) [2,4)]. In these coexisting gases, H_2O and HNO_3 are condensable gases. It is assumed that condensates of the condensable gases are generated and the gaseous Ru migrates to the liquid phase when the temperature of the migration pathway is lower than the dew point. Because gaseous RuO_4 (RuO_4(g)) decomposes more slowly in the gas phase containing HNO_3 or NO_x than in dry air [5,6)], migration to the liquid phase is an important phenomenon in predicting the RuO_4(g) leak path factor (LPF) in a migration pathway [7)].

Sasahira et al. reported that vapor–liquid equilibrium was established when RuO_4(g) migrated to the liquid phase in an aqueous HNO_3 solution [8)]. Conversely, some reports suggested that chemical absorption may occur when nitrous acid (HNO_2, a component formed when NO_x is dissolved in H_2O) is present in the liquid phase. Cains et al. discussed the reaction of RuO_4 with HNO_2 in gas absorption into the liquid phase [9)]. The report of Igarashi et al. showed that absorption rates differ when gas absorption was performed with nitric oxide (NO) or nitrogen dioxide (NO_2) as coexisting gases [10)]. However, there have been few systematic evaluation reports of the effect of HNO_2 on the migration of RuO_4(g) into the liquid phase [9,11,12)].

The purpose of this study is to provide information on the effect of HNO_2 on the migration behavior of RuO_4(g) to the liquid phase. The following three points were evaluated experimentally.

- An experimental apparatus capable of supplying RuO_4(g) at a constant supply rate was prepared, and experiments were conducted to evaluate the absorption ratio of Ru by supplying RuO_4(g) to temperature-controlled gas sample absorbents.
- The experiments were conducted with HNO_2 concentration and temperature as parameters, and systematic data were obtained. As the control, experiments using H_2O as an absorbent were also conducted.
- The ultraviolet/visible (UV/Vis) absorption spectra of the absorbents were obtained, and the reactions involved in chemical absorption were discussed.

The results of this study provide experimental data on the migration of gaseous Ru to condensate, which is important information on the behavior of gaseous Ru in the EDLCF. These data will contribute to the appropriate evaluation of accident consequences and countermeasures of the EDLCF.

2. Materials and methods

2.1 Apparatus

A schematic diagram of the experimental apparatus is shown in **Figure 1.** This apparatus consists of a gaseous RuO_4 generator, an optical system, and a Ru recovery system. The gaseous RuO_4 generator and the optical system were described in previous work [6]. The optical system was used to evaluate the RuO_4(g) supply rate. The vacuum pump and mass flow controller B (MFC-B) were used to regulate the gas flow rate in the apparatus. The air intake was kept open at all times, and the internal pressure of the apparatus was always maintained at atmospheric pressure. The RuO_4(g) supply rate was controlled by adjusting mass flow controller A (MFC-A). By preventing the flow rate of MFC-A from exceeding that of MFC-B, any shortage of airflow was naturally supplied from the air intake, and as a result, a constant flow rate was maintained in the apparatus.

The Ru recovery system consisted of two gas washing bottles connected in series. The first gas washing bottle had the sample absorbent, and the second bottle had 1 mol/L sodium hydroxide solution (NaOH(aq)). The Ru not collected by the first gas washing bottle is completely recovered by the second absorbent.

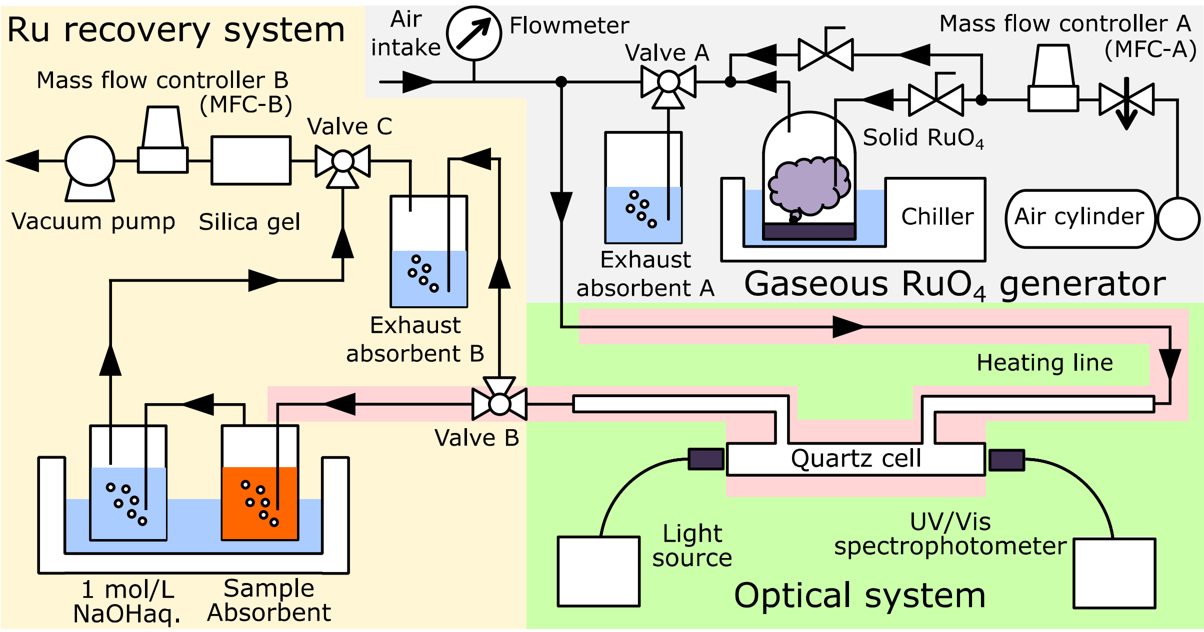

Figure 1 Schematic diagram of the experimental apparatus

The apparatus measures the absorption rate of gaseous RuO_4 into the various gas absorbents. The supply ratio of RuO_4 was measured by the optical system.

2.2 Experimental conditions

The temperature and composition of the sample absorbents are summarized in **Table 1**. In this study, experiments were conducted with the parameters of temperature and HNO_2 concentration. Condensate containing a high concentration of HNO_3 (>2 mol/L) can be generated during EDLCF. However, a high concentration of HNO_3 was not used in this study because HNO_3 is decomposed to form HNO_2. A concentration of twice the highest HNO_2 concentration in the experimental condition was adopted as the concentration of HNO_3. The experiments with water (Run 4-1, Run 30-1, and Run 50-1) were control experiments for measuring the effect of HNO_3. Sodium nitrite ($NaNO_2$) was used as the HNO_2 source. Other experimental conditions are summarized in the supporting information (Appendix **Table A**, **B**, and **Fig. A**). Because the rate of RuO_4(g) generation decreases with time, the value of MFC-A was gradually increased as needed to keep the supply rate as constant as possible.

Table 1 Composition of sample absorbents and temperature of the experiments

Experiment I.D.	Temperature (°C)	HNO_3 (mmol/L)	$NaNO_2$ (mmol/L)
Run 4-1	4	0	0
Run 4-2	4	100	0
Run 4-3	4	100	1
Run 4-4	4	100	5
Run 4-5	4	100	10
Run 4-6	4	100	17.5
Run 4-7	4	100	25
Run 4-8	4	100	37.5
Run 4-9	4	100	50
Run 30-1	30	0	0
Run 30-2	30	100	0
Run 30-3	30	100	0.5
Run 30-4	30	100	1
Run 30-5	30	100	2.5
Run 30-6	30	100	5
Run 30-7	30	100	7.5
Run 30-8	30	100	10
Run 50-1	50	0	0
Run 50-2	50	100	0
Run 50-3	50	100	0.5
Run 50-4	50	100	1
Run 50-5	50	100	1.5
Run 50-6	50	100	2.5
Run 50-7	50	100	5

2.3 Definition of Ru absorption ratio

An index indicating the Ru absorption activity of the absorbents, the Ru absorption ratio, was defined as Eq.(1) and used to compare each experimental result.

$$\text{Ru absorption ratio (\%)} = \text{Ru}_{\text{abs}}/(\text{Ru}_{\text{abs}} + \text{Ru}_{\text{NaOH(aq)}}) \times 100 \quad (1)$$

where Ru_{abs} is the amount of Ru collected in sample absorbent (mol), $Ru_{NaOH(aq)}$ is the amount of Ru collected in NaOH(aq) (mol).

2.4 Experimental procedure

A Solid RuO_4 was incubated at −10 °C for 30 min in a chiller to reach a constant temperature. To adjust the zero value of the spectrophotometer, 0.5 NL/min of air was supplied to the quartz cell from the air intake using the vacuum pump. Simultaneously, valve A was adjusted to supply RuO_4(g) to the exhaust absorbent A for a few minutes while the RuO_4(g) generation rate stabilized.

After that, valves A, B, and C were switched to allow the RuO_4(g) to pass through the quartz cell to the exhaust absorbent B. The flow rate of MFC-A was adjusted so that the supply rate of RuO_4(g) was the same in each experiment. Subsequently, valves B and C were switched to supply RuO_4(g) to the sample absorbent and NaOH(aq).

After RuO_4(g) was supplied for 15 min, valves B and C were switched again to supply RuO_4(g) to the exhaust absorbent B. The immobilization agent (20 mL of 3.0 mol/L NaOH solution) was added to prevent re-volatilization of the RuO_4(g) from the sample absorbent. If the black precipitate presumed to be ruthenium dioxide (RuO_2) was observed, potassium peroxodisulfate ($K_2S_2O_8$) was added to the sample absorbent as a solubilizing agent. After that, 15 mL of absorbent were sampled. Ru in each sample was quantitatively analyzed using inductively coupled plasma mass spectrometry (Perkin-Elmer, DRC-e).

3. Results and discussion

3.1 Comparison of Ru absorption ratio for each sample absorbent

The Ru absorption ratios obtained in each experiment are compared in **Figure 2.** Other detailed results have been summarized in **Table 2**. The Ru absorption ratio tended to increase at higher HNO_2 concentrations.

At lower HNO_2 concentrations (0–1 mmol/L), the Ru absorption ratio was higher at lower temperatures. A trend of these results is the same as that in the gas–liquid equilibrium experiments conducted by Sasahira et al. [8]. Conversely, when the HNO_2 concentration was high (≥1.5 mmol/L), the Ru absorption rate was higher at higher temperatures. In the experiments at 30 °C and 50 °C, almost all of the RuO_4(g) was collected with 2.5 mmol/L HNO_2, whereas in the experiment at 4 °C, 3.2% of the RuO_4(g) passed through the sample absorbent even when 50 mmol/L of HNO_2 was used as the sample absorbent. **Figure 3** shows the relationship between the Ru absorption ratio and the absorbent temperature at each HNO_2 concentration. At the experiments with low HNO_2 concentrations (0 mM, 0.5 mM, and 1.0 mM), the Ru absorption ratio decreased with increasing temperature. On the other hand, when the HNO_2 concentration was high (2.5 mM and 5 mM), the Ru absorption ratio increased with increasing temperature. We considered that, at low HNO_2 concentration, the Ru absorption ratio decreased as a result of the decrease in gas solubility with increasing temperature. In contrast, at high HNO_2 concentrations, the trend was reversed because the effect of chemical absorption was accelerated with increasing temperature.

These results indicate that chemical absorption involving HNO_2 and RuO_4 occurs. It is considered that the higher temperature yields a higher Ru absorption ratio because of the activation of reactions involved in the chemical absorption of RuO_4(g) when HNO_2 is in the liquid phase.

It is important to note that even in the experiments using H_2O as the sample absorbent, the majority of Ru was absorbed (Run 4-1, Run 30-1, and Run 50-1). It is assumed that the migration of RuO_4(g) into the condensate has a large effect on the LPF of Ru in an EDLCF.

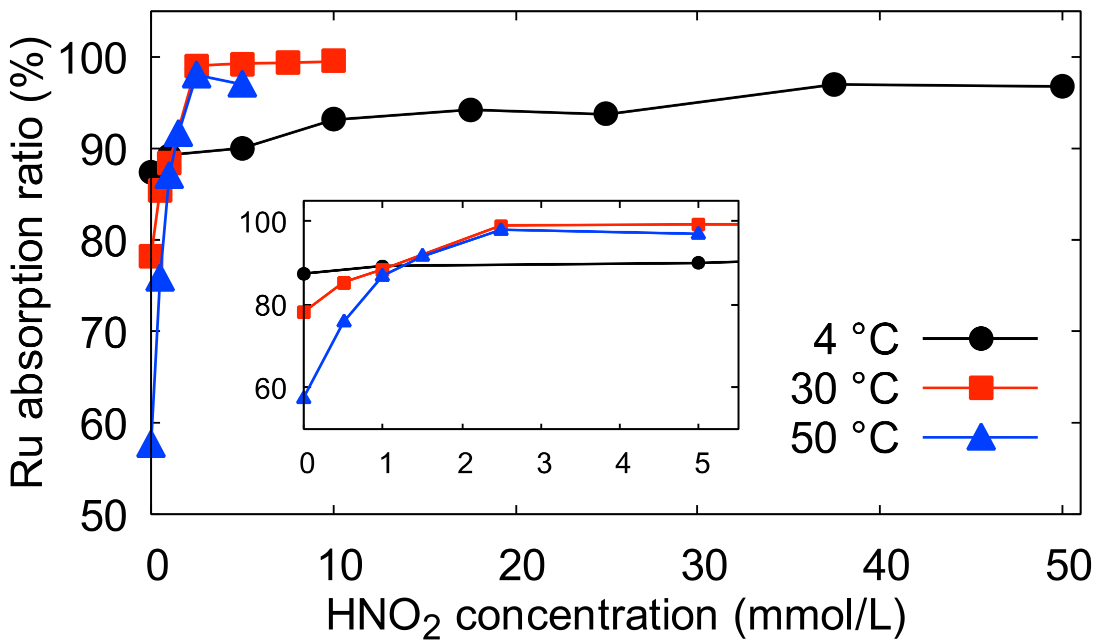

Figure 2 Relationship between Ru absorption ratio and HNO_2 concentration

The value of Ru absorption ratio was calculated from Eq. 1. The inset graph is an enlarged plot of the region of HNO_2 concentration 1-5 mmol/L.

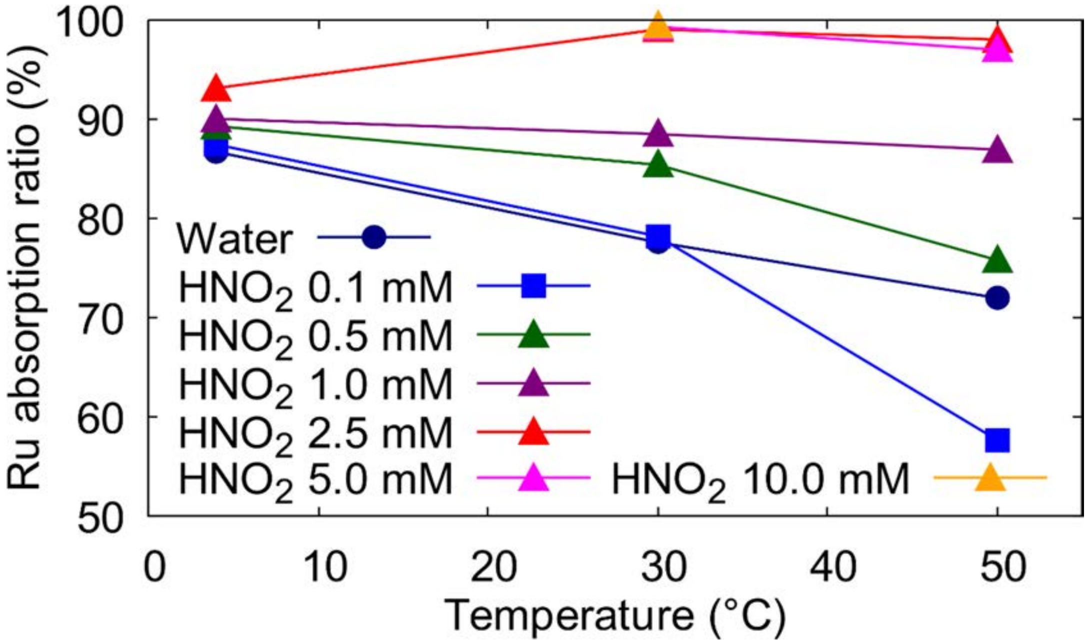

Figure 3 Relationship between Ru absorption ratio and temperature

The value of Ru absorption ratio was calculated from Eq. 1. The Ru absorption ratio decreased with increasing temperature when HNO_2 concentration absorbent was low. Conversely, when HNO_2 concentration was high, an increase in the Ru absorption ratio with increasing temperature was observed.

Table 2 Summary of experimental results

Run	Aeorbent	Absorbent amout (mL)	Flow rate (NL/min)	Ru supply time (min)	Temperature (℃)	Peak area of absorbance at 306 nm	Ru in Sample Absorbent (ppb)	Ru in Sample Absorbent (μg)	Ru in Sample Absorbent (μmol)	Ru in NaOHaq (ppb)	Ru in NaOHaq (μmol)	Total Ru (μmol)	Total Ru (mg) as RuO_4	RuO_4(g) conc. (mg/L)	RuO_4(g) conc. (%)	RuO_4(g) conc. (ppm)	Ru supply rate (μmol/min)	Ru absorption ratio (%)	Black Precipitate
Run 4-1	Water	300	0.5	15	4	200602.4	16217	4865.1	48.16	2484	7.38	55.54	9.2	18.3	0.25	2524	3.70	**86.7**	-
Run 4-2	0.1 mol/L HNO_3	300	0.5	15	4	205823.1	17104	5131.2	50.79	2453	7.28	58.08	9.6	19.2	0.26	2640	3.87	**87.5**	-
Run 4-3	1 mmol/L HNO_2	300	0.5	15	4	213549.5	17588	5276.4	52.23	2107	6.26	58.49	9.7	19.3	0.27	2659	3.90	**89.3**	+
Run 4-4	5 mmol/L HNO_2	300	0.5	15	4	211042.2	17820	5346.0	52.92	1971	5.85	58.77	9.7	19.4	0.27	2672	3.92	**90.0**	+
Run 4-5	10 mmol/L HNO_2	300	0.5	15	4	217892.8	19883	5964.9	59.05	1465	4.35	63.40	10.5	20.9	0.29	2882	4.23	**93.1**	-
Run 4-6	17.5 mmol/L HNO_2	300	0.5	15	4	211749.2	20848	6254.4	61.91	1273	3.78	65.69	10.8	21.7	0.30	2986	4.38	**94.2**	-
Run 4-7	25 mmol/L HNO_2	300	0.5	15	4	228449.2	19674	5902.2	58.43	1317	3.91	62.34	10.3	20.6	0.28	2834	4.16	**93.7**	-
Run 4-8	37.5 mmol/L HNO_2	300	0.5	15	4	233255.4	22135	6640.5	65.73	684	2.03	67.77	11.2	22.4	0.31	3080	4.52	**97.0**	-
Run 4-9	50 mmol/L HNO_2	300	0.5	15	4	233001.5	21934	6580.2	65.14	730	2.17	67.31	11.1	22.2	0.31	3059	4.49	**96.8**	-
Run 30-1	Water	300	0.5	15	30	211379.6	13888	4166.4	41.24	4008	11.90	53.15	8.8	17.5	0.26	2643	3.54	**77.6**	-
Run 30-2	0.1 mol/L HNO_3	300	0.5	15	30	204156.3	13656	4096.8	40.55	3802	11.29	51.85	8.6	17.1	0.26	2578	3.46	**78.2**	-
Run 30-3	0.5 mmol/L HNO_2	300	0.5	15	30	206741.7	15469	4640.7	45.94	2641	7.84	53.78	8.9	17.8	0.27	2674	3.59	**85.4**	+
Run 30-4	1 mmol/L HNO_2	300	0.5	15	30	207193.9	15702	4710.6	46.63	2039	6.06	52.69	8.7	17.4	0.26	2620	3.51	**88.5**	-
Run 30-5	2.5 mmol/L HNO_2	300	0.5	15	30	207488.4	17822	5346.6	52.93	171	0.51	53.43	8.8	17.6	0.27	2657	3.56	**99.0**	-
Run 30-6	5 mmol/L HNO_2	300	0.5	15	30	212793.2	18664	5599.2	55.43	130	0.39	55.81	9.2	18.4	0.28	2775	3.72	**99.3**	-
Run 30-7	7.5 mmol/L HNO_2	300	0.5	15	30	214890.8	18806	5641.8	55.85	118	0.35	56.20	9.3	18.6	0.28	2794	3.75	**99.4**	-
Run 30-8	10 mmol/L HNO_2	300	0.5	15	30	220654.9	19589	5876.7	58.17	99	0.29	58.47	9.7	19.3	0.29	2907	3.90	**99.5**	-
Run 50-1	Water	300	0.5	15	50	219636.4	13459	4037.7	39.97	5234	15.54	55.51	9.2	18.3	0.29	2942	3.70	**72.0**	-
Run 50-2	0.1 mol/L HNO_3	300	0.5	15	50	231777.2	10638	3191.4	31.59	7800	23.16	54.76	9.0	18.1	0.29	2902	3.65	**57.7**	-
Run 50-3	0.5 mmol/L HNO_2	300	0.5	15	50	245559.1	14706	4411.8	43.67	4691	13.93	57.60	9.5	19.0	0.31	3053	3.84	**75.8**	+
Run 50-4	1 mmol/L HNO_2	300	0.5	15	50	257359.6	17364	5209.2	51.57	2607	7.74	59.31	9.8	19.6	0.31	3144	3.95	**86.9**	-
Run 50-5	1.5 mmol/L HNO_2	300	0.5	15	50	258326.3	19219	5765.7	57.07	1766	5.24	62.32	10.3	20.6	0.33	3303	4.15	**91.6**	-
Run 50-6	2.5 mmol/L HNO_2	300	0.5	15	50	263778.7	17999	5399.7	53.45	361	1.07	54.52	9.0	18.0	0.29	2890	3.63	**98.0**	-
Run 50-7	5 mmol/L HNO_2	300	0.5	15	50	263853.4	20476	6142.8	60.81	630	1.87	62.68	10.3	20.7	0.33	3322	4.18	**97.0**	-

3.2 Chemical form of Ru in the sample absorbents

The UV/Vis spectra of the sample absorbents were measured after RuO_4(g) supply (**Figure 4**). For H_2O (Run 4-1), the spectrum of dissolved RuO_4 was clearly observed, indicating that the supplied RuO_4 retained its chemical form (**Figure 4**) [13]. For HNO_3(aq) (Run 4-2), the absorption of RuO_4 and HNO_3 overlapped at approximately 300 nm; however, the absorption at approximately 390 nm is similar to that of H_2O. This result suggests that RuO_4 retains its chemical form in HNO_3(aq). Conversely, in the sample absorbent containing 1 mmol/L HNO_2 (Run 4-3), the spectrum of RuO_4 disappeared, indicating that RuO_4 reacted with HNO_2 to change to different chemical forms, such as RuO_2 and ruthenium(III) nitrosyl nitrate complexes (Ru(III), such as $Ru(NO)(NO_3)$) (Eq. (2) and Eq. (3)). The black precipitate presumed to be RuO_2 was indeed observed in some of the sample absorbents (**Table 2**). This result is similar to the results in the report of Cains et al. [9].

$$RuO_4 + 2HNO_2 \rightarrow RuO_2 + 2HNO_3 \qquad (2)$$

$$RuO_4 + 4HNO_2 \rightarrow Ru(NO)(NO_3)_3 + 2H_2O \qquad (3)$$

In experiments with HNO_2, the UV/Vis absorption spectra corresponding to the Ru(III) could not be observed because of the measurement interference by HNO_2 (Appendix **Fig. B**). However, the precipitate presumed to be RuO_2 was not observed in the sample absorbents with relatively high HNO_2 concentration, indicating that the Ru(III) may preferentially form in these absorbents.

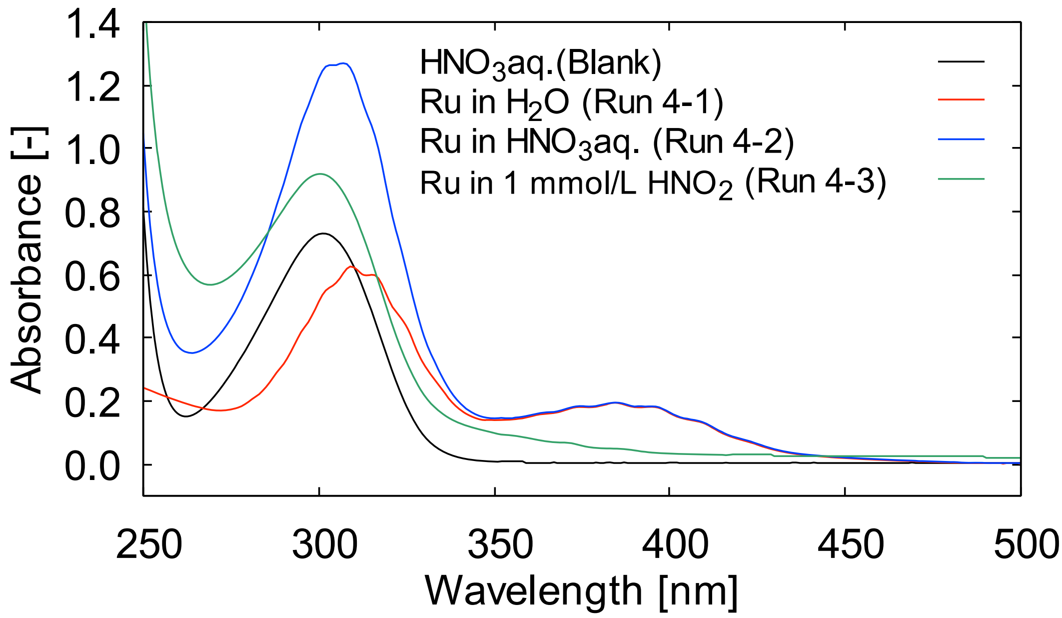

Figure 4 Effect of HNO_2 on chemical form of Ru in sample absorbents

Considering the UV absorption at 350 -400 nm, the RuO_4 retained its chemical form when H_2O (red line) or HNO_3(aq) (blue line) was used as the absorbent. On the other hand, in the presence of HNO_2, the absorption of RuO_4 disappeared (green line).

4. Conclusion

In this study, $RuO_4(g)$ gas absorption experiments were conducted with temperature and HNO_2 concentration as parameters. Chemical absorption effects of HNO_2 were as follows:

- The Ru absorption ratio rose with increasing HNO_2 concentration in the sample absorbents, indicating the presence of chemical absorption involving HNO_2.
- In the experiments with absorbent HNO_2, the Ru absorption ratio rose with increasing temperature. The reactions involved in the chemical absorption were considered to be activated by temperature.

These results may contribute to the improvement of accident management measures and source term analysis of the EDLCF by improving the accuracy of prediction of Ru migration behavior.

Acknowledgements

The authors wish to thank Mr. T. Masaki, Mr. R. Saito, Mr. T. Ito, and all members of the Fuel Cycle Research Group of Japan Atomic Energy Agency who provided technical help.

References

1) Nuclear Regulation Authority (Japan), Outline of the Draft New Regulatory Requirements for Nuclear Fuel Facilities, Research Reactors, and Nuclear Waste Storage/Disposal Facilities, 2013, Available from: https://www.nsr.go.jp/data/000067274.pdf (accessed 2021-05-11).
2) Philippe, M. et al., Behavior of ruthenium in the case of shutdown of the cooling system of HLLW storage tanks, Proceedings of 21st DOE/NRC Nuclear Air Cleaning Conference, San Diego, 1990, pp. 831-843.
3) Miyata, T. et al., Application of Probabilistic Safety Assessment to Rokkasho Reprocessing Plant, (II) The Occurrence Frequency of Boiling Accident of Highly Active Liquid Waste, Trans. At. Energy. Soc. Japan., vol.7, no.2, 2008, pp.85-98.
4) Tashiro, S. et al., Release of Radioactive Materials from Simulated High-Level Liquid Waste at Boiling Accident in Reprocessing Plant, Nucl. Technol., vol.190, no.2, 2015, pp.207-213.
5) Yoshida, N. et al., Migration behavior of gaseous ruthenium tetroxide under boiling and drying accident condition in reprocessing plant, J. Nucl. Sci. Technol., vol.55, no.6, 2018, pp.599-604.
6) Yoshida, N. et al., Decomposition behavior of gaseous ruthenium tetroxide under atmospheric conditions assuming evaporation to dryness accident of high-level liquid waste, J. Nucl. Sci. Technol., vol.57, no.11, 2020, pp.1256-1264.
7) U.S. Department of Energy (DOE), Airborne release fractions / rates and respirable fractions for nonreactor nuclear facilities volume I - Analysis of experimental, DOE-HDBK-3010-94 Volume I (Reaffirmed 2013), 1994, 359p.

8) Sasahira, A., Kawamura, F., Formation rate and gas-liquid equilibrium of RuO_4, J. Nucl. Sci. Technol., vol.25, no.5, 1988, pp.472-478.

9) Cains, P.W. et al., Absorption of volatile ruthenium, AERE-R-13197, 1988, 56p.

10) Igarashi, H. et al., Absorption Behaviour of Gaseous Ruthenium into Water, Radiochim. Acta, vol.57, no.1, 1992, pp.51-55.

11) Shibata, Y. et al., Evaluation of RuO_4 absorption to the water, Proceedings of Atomic Energy Society of Japan 2016 Annual Meeting, Sendai, 2016, 3P11.

12) Kinuhata, H. et al., Experiment to measure the absorption rate coefficient of volatile Ru in the condensate, Proceedings of Atomic Energy Society of Japan 2020 Annual Meeting, Fukushima, 2020, 2E09.

13) Barton, G.B., The ultraviolet absorption spectrum of ruthenium tetroxide, Spectrochim. Acta., vol.19, no.9, 1963, pp.1619-1621.

Appendix

Supporting information

1 Experimental condition

Table A Parameters for experimental apparatus operation

Parameter	Value
RuO_4 chiller (℃)	-10
MFC-A (NL/min)	0.2-0.4
MFC-B (NL/min)	0.5
Optical path length (cm)	25
Sample absorbent (mL)	300
1.0 mol/L NaOHaq. (mL)	300
Sampling time (min)	15

2 Standard curve of Ru supply

In order to measure the supply rate of the RuO_4(g), a standard curve was prepared using the data of the peak area in the time course of absorbance at 306 nm, which is the local maximum absorption wavelength of the RuO_4(g), and the actual amount of supplied Ru (Table A and Table B). The peak areas were calculated by using "Measure Path" function of the Inkscape software.

Table B Standard curve between Ru supply rate and peak area of absorbance at 306 nm

RuO_4(g) carrier gas (MFC-A) (NL/min)	Absorbent amount (mL)	Peak area of absorbance at 306 nm	Ru in NaOHaq (ppb)	Ru in NaOHaq (μmol)	Ru supply time (min)	Ru supply rate (μmol/min)
0.02	300	12040.2	1159	3.44	10	0.34
0.05	300	24426.6	2247	6.67	10	0.67
0.1	300	62473.1	5678	16.86	10	1.69
0.15	300	97174.4	8896	26.42	10	2.64
0.2	300	134697.4	12214	36.27	10	3.63
0.25	300	174112.3	15920	47.28	10	4.73

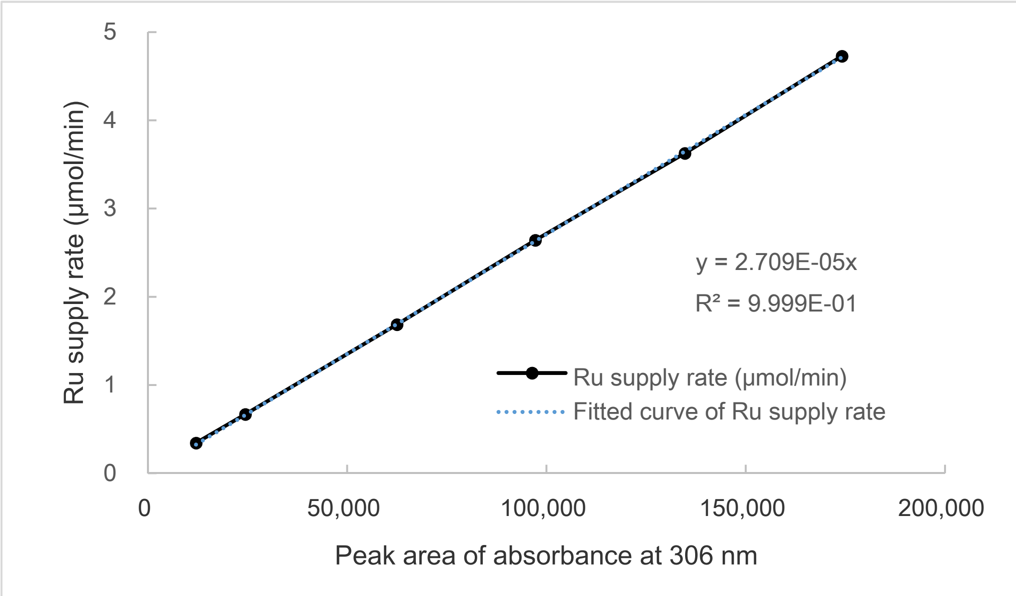

Fig. A Standard curve of Ru supply rate

3 UV/Vis absorption spectra of sample absorbents containing HNO_2

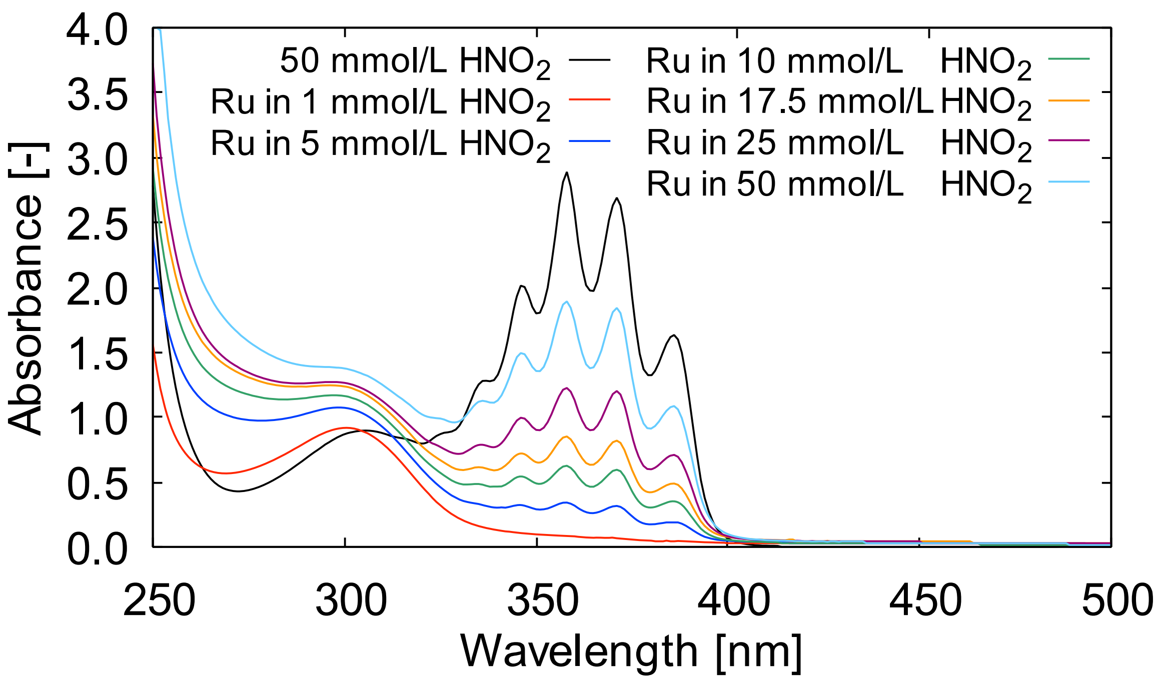

Fig. B UV/Vis absorption spectra of sample absorbents containing HNO_2